Effects of filling fluid type and composition and joint orientation on acoustic wave propagation across individual fluid-filled rock joints

Hui YANG (Yang H.) [a,b], Huan-feng DUAN (Duan H.F.) [a,b], Jianbo ZHU (Zhu J.B.) [c,*]

[a] Department of Civil and Environmental Engineering, The Hong Kong Polytechnic University, Hong Kong SAR
[b] Research Institute for Sustainable Urban Development, The Hong Kong Polytechnic University, Hong Kong SAR
[c] State Key Laboratory of Hydraulic Engineering Simulation and Safety, School of Civil Engineering, Tianjin University, Tianjin, China
* Corresponding author, Email: jbzhu@tju.edu.cn;

Abstract:

Wave propagation and attenuation in subsurface rock masses could be highly affected by rock joints filled with fluids. However, the understanding of acoustic behaviours across fluid-filled rock joints is still at its infancy. To determine the effects of the type and composition of filling fluids as well as joint orientation on compressional wave propagation and attenuation across individual fluid-filled rock joints, extensive laboratory acoustic tests were conducted in this paper. Results showed that the existence of water in fluid-filled rock joints results in higher wave velocity, more wave transmission and less wave attenuation compared to light oils. In most circumstances, increasing liquid content in a single-liquid filled joint enhances wave velocity and wave transmission. For dual-liquid filled joints, both wave velocity and wave transmission increase with increasing water content. Joint orientation significantly affects wave characteristics of rock joints partially filled with liquids while it has slight influences on wave attributes of rock joints fully filled with liquids. In addition, wave velocity and attenuation across fluid-filled rock joints increases with increasing central frequency of incident compressional waves.

Keywords:

Fluid; Rock joint; Joint orientation; Wave propagation

1. Introduction

The presence of fluids in rock discontinuities at different scales, e.g., joints, could strongly affect acoustic wave propagation in the Earth's crust [1]. Understanding wave responses to fluid-filled rock joints is of great importance to many kinds of practical engineering applications, such as reservoir detection and characterization, geothermal exploration and extraction, underground engineering appraisal, exploration seismology and earthquake engineering [2-6]. For instance, seismic wave attenuation and velocity can be used to determine the fracture specific stiffness, which is a key parameter to characterize alternations of a facture induced by fluid flow [7]. Despite of previous studies on wave properties of individual water-filled rock joints, the understanding of wave behaviours across fluid-filled rock joints is still at infancy. Specifically, effects of filling fluid parameters (e.g., type, composition and distribution) and joint features (such as joint orientation and joint roughness) on wave propagation in jointed rock masses are still not well understood. Therefore, it is necessary to further investigate wave propagation through fluid-filled rock joints.

In respect of theoretical analysis, there are two common theories for analysing wave propagation across individual fluid-filled rock joints. The first one is the linear slip theory (LST), in which the stress is assumed to be continuous while the displacement is treated as discontinuous across the joint [8-9]. The LST was combined with a velocity discontinuity by Pyrak-Nolte et al. to derive complete solutions for P- and S-waves incidence upon a fracture saturated with liquid [10]. Despite of its simple form and effectiveness, the LST is only applicable for the joint with aperture much smaller than the incident wavelength [11]. The other one is the layered medium theory (LMT) where the joint is modelled as a thin plane layer and displacements and stresses are assumed to be continuous across its two interfaces [12]. Different from the LST, LMT is capable of analysing wave responses to rock joints regardless of the relation between the joint aperture and the wavelength [13-16]. Based on the LMT, Fehler derived transmission and reflection coefficients for P, SV, and SH waves incident at arbitrary angles onto a viscous fluid layer embedded between two homogeneous half-spaces [17]. Recently, Zhu et al. improved LMT to compute theoretical solutions for wave propagation across viscoelastic filled joints [18], and Zhu et al. suggested that the more viscous the filled medium is, the less the wave energy transmits across the joint [19]. Oelke et al. derived full analytical solutions of reflection coefficients for P- and S-waves impinging on a fracture filled with a thin ideal fluid layer [20]. The thin ideal fluid layer is supposed to represent a planar

layer of a non-viscous fluid, where the layer thickness is much smaller than the wavelength of incident wave.

In addition to theoretical investigations, some experimental studies have been conducted to better understand the interaction of wave propagation with individual fluid-filled rock joints. The preliminary laboratory results of Pyrak-Nolte et al. suggested that filling fluids could increase spectral amplitudes of transmitted P- and S-waves across a fracture, where the increment for P-wave is much greater than that for S-wave [10]. Minato and Ghose conducted ultrasonic tests on single dry and water-filled fractures and stated that the calculated fracture compliance ratio from the P-P and P-S amplitude-versus-offset (AVO) inversion could be applied to accurately estimate the existence of fluid in the fracture [21]. Additionally, Place et al. carried out ultrasonic tests on an artificial fracture filled with various fluids, where the filling fluid was almost at rest in the fracture or moving at a controlled flow rate through the fracture [22]. They found that the types of fluids could highly affect reflected wave spectra and energy, while the internal fluid flow has negligible influences on wave reflection. Recently, Kamali-Asl et al. examined ultrasonic P- and cross-polarized S-wave responses to a fluid-filled rock fracture using the pressure- and displacement-controlled flow-through-fracture tests, where waves propagate along the direction of flow in the joint. The test results indicated that P-wave velocity and attenuation as well as the maximum amplitude of S waves could characterize changes in fracture aperture induced by the fluid flow [23]. More recently, Yang et al. carried out a series of ultrasonic tests on single natural joints filled with water using incident P-waves with different frequencies [24]. Their results suggested that increasing water volume content in the joint or decreasing joint thickness may reduce wave attenuation but improve wave velocity and wave transmission. Nonetheless, the effects of the other in-situ conditions, e.g., type and composition of filling fluids as well as joint orientations, on wave behaviours across fluid-filled joints are still not well determined. Therefore, further efforts are needed to fill the knowledge gap in the interaction of acoustic waves with fluid-filled rock joints.

To examine compressional wave propagation and attenuation across individual fluid-filled rock joints with different types and compositions of filling fluids as well as joint orientations, a series of ultrasonic tests across fluid-filled rock joints were carried out in current study. On the basis of the laboratory data, the key wave attributes, i.e., wave velocity, frequency spectra, transmission coefficient and attenuation quality factor Q, were evaluated to quantitatively determine the influences of filling fluid parameters and joint orientation on wave behaviours. The physical mechanisms lying behind these results were further analysed and

discussed in terms of acoustic properties of rock discontinuities and filling fluids. The findings in the present study are of great importance to get deeper insights into wave propagation and attenuation through rock joints.

2. Experimental set-up

2.1 Sample preparation

The rock samples for this study were manufactured using the high-quality black gabbro produced in Shanxi, China, as shown in Fig. 1a. The black gabbro rock was chosen for this investigation because of its good integrity and homogeneity. Hence wave attenuation and slowness caused by gabbro rock matrix is negligible compared with those caused by rock joints, thereby highlighting the influence of rock joints on wave propagation in this study. The mineralogical components of the gabbro (see Fig. 1b) are plagioclase (75%), clinopyroxene (20%), quartz (3%), amphibole (1%) and biotite (1%). The grain sizes of this rock are in the range of 0.05–2 mm, which are determined by making a modal analysis on a rock slab using a petrographic microscope. The other physical and mechanical properties of the gabbro were measured and listed in Table 1.

In this study, an open rock joint was firstly manufactured by combining two identical rock cylinders using a PMMA tube, where 3M DP460NS epoxy adhesive was utilized to stick the tube and two rock cylinders together, as shown in Fig. 1a. These rock cylinders were 50 mm in diameter and 50 mm in height. The PMMA tube was used to not only connect these two intact rock cylinders but also prevent the outflow of filling fluids with the help of sealing layer produced by the epoxy adhesive. Moreover, a pre-set hole with a diameter of 2 mm on the PMMA tube was made for injecting fluids into the open rock joint. The length of this artificially jointed rock sample was measured to be around 106 mm, and hence the thickness (aperture) of the artificial joint sandwiched between two rock cylinders was about 6 mm. Using the artificial open joint, a series of fluid-filled rock joints were then prepared by injecting fluids into the joint aperture through the pre-set hole on the tube. In this study, filling fluids include air, water and two types of light oils, i.e., Shell Morlina S2 BL10 and Shell Tellus S2 M68 (see Fig. 1c). For convenience, Shell Morlina S2 BL10 and Shell Tellus S2 M68 are abbreviated to BL10 and M68 respectively in this study. The properties of different fluids at room temperature are shown in Table 2, among which attributes of two light oils were measured carefully in the laboratory [25-26].

Table 3 lists all filling conditions of fluid-filled rock joints considered in this study. Herein, three types of liquids, i.e., water, BL10 and M68, were injected into the joint in

different combination modes to prepare multiple fluid-filled joints (with clear fluid stratification rather than mixed fluid). For clarity, all testing cases can be divided into two groups, i.e., group A for the single-liquid filled joint that is filled with air and one kind of liquid, and group B for the dual-liquid filled joint that is fully filled with two kinds of liquids. Since the joint spatial orientation might affect the distribution and stratification of fluids in the joint, fluid-filled joints at both vertical and horizontal orientations (corresponding to joint dip angles of 90° and 0°, respectively, for in-situ condition) were tested in each group.

In addition, two types of incident waves with central frequencies of 100 kHz and 1 MHz were applied to study the effects of incident wave bandwidth on wave propagation and response through individual fluid-filled rock joints. To quantitatively analyse wave responses to fluid-filled rock joints, an intact rock sample with the same size as the jointed rock sample was prepared to obtain reference data (see Fig. 1a). Note that end surfaces of all cylindrical rock samples used in this study were ground flat, smooth and parallel within 0.01mm. Besides, a cylindrical aluminium sample of the same dimensions was also prepared, which would be used to provide the reference frequency spectra for effective evaluation and analysis of wave attenuation in jointed rock samples. To guarantee the repeatability and effectivity of all the above testing cases in this study, five tests were conducted for each case to minimize the system noises and operation errors.

2.2 Experimental apparatuses

In this study, the pulse transmission method was used to take acoustic measurements on jointed and intact rock samples [27]. As illustrated in Fig. 2, the test rig consists of an ultrasonic test system and a uniaxial loading system. The ultrasonic system in Fig. 2a is composed of a Tektronix digital oscilloscope (model DPO 2012B), an Olympus pulser/receiver (model 5077PR), a pair of ultrasonic transducers (i.e., a transmitter and a receiver) and a personal computer (PC). For each measurement, the transmitter was excited by a 200-Voltage spike with a duration of 10 μs at a repetition rate of 100 Hz generated by the Olympus pulser/receiver, which then sent the simultaneous pulses into the tested specimen. After propagating through the rock sample, the transmitted signal was detected and captured by the receiver connected to the Olympus pulser/receiver. Connected to the Olympus pulser/receiver, the oscilloscope was used to digitize, display and record a portion of each transmitted signal with a duration of 120 μs at a sample interval of 0.001 μs. During each test, 64 digitized transmitted pulses were stacked to produce a high signal-to-noise ratio and to obtain steady test results. The received data were saved on a hard disk through the PC equipped with a data acquisition software. In

this study, two pairs of Olympus P-wave transducers with different natural frequencies, i.e., model X1020 (100 kHz) and model V192 (1 MHz), were used to investigate the effects of incident waves at different dominant frequencies on wave behaviours across fluid-filled rock joints. Using the method recommended in ASTM Standard D2845-08 [28], the delay time caused by structures of transducers was measured to be 1.172 ± 0.105 μs and 0.360 ± 0.021 μs for P-100 kHz and P-1 MHz transducers, respectively.

The loading system, consisting of a loading cell, a pump and a steel frame (see Fig. 2b), was utilized to impose a constant external axial stress (about 0.064 MPa) to the combination of the rock specimen and the transducers, thereby enhancing the coupling of their interfaces and increasing the stability of the test system. Besides, Vaseline was used on the rock-transducer interface for compactly coupling their end surfaces. As illustrated in Fig. 2b, the loading system and the rock sample were horizontally placed when studying wave propagation across vertical fluid-filled rock joints. In comparison, to measure wave attributes of horizontal fluid-filled rock joints, both the loading system and the rock sample were vertically arranged. Note that the experimental setup would be disassembled and then reassembled to examine the signal reproducibility between the adjacent measurements, so as to reduce as much as possible the errors during the tests.

3. Data processing and analysis methods

3.1 Wave velocity

According to ASTM Standard D2845-08 [28], wave velocity in the jointed rock sample can be calculated by

$$V = \frac{L}{t} \tag{1}$$

where L is the total length of the rock sample measured by a Vernier calliper with an accuracy of 0.01mm, and t is the travel time of wave through the rock sample determined by subtracting the delay time of transducers (t_d) from the measured arrival time of wave through the rock specimen (t_a). For propagating waves with high-frequency and short-wavelength, the travel time of wave through the jointed rock sample is equivalent to the cumulative travel time of wave through rock matrix and the joint [29]. Accordingly, the relationship among wave velocities of the whole jointed rock sample, the rock matrix and the rock joint could be described by Wyllie's time-average equation as follow [30]

$$V = \frac{L}{t_r + t_j} = \frac{L_r + L_j}{\dfrac{L_r}{V_r} + \dfrac{L_j}{V_j}} \qquad (2)$$

where t_r and t_j are travel time of waves across the rock matrix and the rock joint, respectively; L_r and L_j are the length of the rock matrix and the rock joint, respectively; V_r and V_j are wave velocities in the rock matrix and the rock joint, respectively. Based on Eq. (2), to better understand the effects of single fluid-filled rock joints on wave properties in this study, wave velocity in the rock joint can be computed by

$$V_j = \frac{L_j}{t - \dfrac{L_r}{V_r}} \qquad (3)$$

3.2 Wave transmission

When evaluating wave transmission through rock joints, the transmitted wave through an intact rock sample is regarded as the reference incident pulse to eliminate effects of micro-pores and micro-cracks as well as interfaces between the rock sample and transducers on wave propagation [10, 31]. Wave transmission is commonly characterized by the transmission coefficient, which is defined as the ratio between amplitudes of the transmitted and incident waves [32]. Herein, transmission coefficient could be calculated using peak-to-peak amplitudes of the first arriving pulses as suggested in the literature [33-35]

$$T = \frac{A_t}{A_i} \qquad (4)$$

where A_t and A_i are the peak-to-peak amplitudes of initial wave transmitted through the jointed rock sample and the intact rock sample, respectively. Note that the peak-to-peak amplitude is the voltage difference between the crest to the trough of the first arriving pulse [33-35].

3.3 Spectral analysis

Spectral analysis is essential to study wave propagation and attenuation since it provides information on wave energy distribution over frequency range [36]. The transmitted waveform is comprised of the initial pulse and subsequent contents possibly contaminated by reflections from various interfaces in the system, where the initial pulse is of great importance to the determination of wave characteristics of rock joints [10, 31]. Thus, spectral analysis is usually conducted on initial pulses to understand wave behaviours through rock joints in the frequency

1 domain. To extract initial pulses from transmitted waveforms, appropriate window functions

2 need to be selected and applied to taper transmitted signals. The criteria for determining

3 appropriate tapers are to alter less spectra of target pulses and to preserve more low-frequency

4 content of transmitted signals without too much distortion in the high-frequency range [10, 31].

5 In this study, by trial and error, a half-cosine taper with an 8.0-μs window and unity amplitude

6 was applied to all transmitted pulses from 100-kHz input signals, and a half-cosine taper with

7 a 3.5-μs window and unity amplitude was applied to all transmitted pulses from 1-MHz

8 incident waves. Fig. 3 illustrates examples of isolating initial signals from the received waves

9 using the selected tapers. Following that, the fast Fourier transform was performed on these

10 tapered initial pulses to calculate their corresponding frequency spectra.

11

12 *3.4 Wave attenuation*

13 Wave attenuation in rock masses is usually quantified by the attenuation quality factor Q. In

14 this paper, Q values of rock samples were determined using the spectral ratio method presented

15 by Toksöz et al., where the ratio of spectral amplitudes is expressed as [37, 38]

16 $$\frac{A_1}{A_2} = \frac{G_1}{G_2} e^{-(\gamma_1 - \gamma_2)fx} \text{ or } \ln(\frac{A_1}{A_2}) = \ln(\frac{G_1}{G_2}) + (\gamma_2 - \gamma_1)fx \tag{5}$$

17 where $A(f)$ is the spectral amplitude, f is frequency, $G(x)$ is the geometric factor related to

18 spreading, reflections, transducer-to-sample bond effect, etc., x is the length of wave travel

19 path (i.e., the sample length), γ is a constant related to Q (i.e., $Q = \frac{\pi}{\gamma v}$), and v is the phase

20 velocity. Subscripts 1 and 2 denote the reference and the rock sample, respectively. The

21 $(\gamma_2 - \gamma_1)$ can be determined by the slope of the line fitted to $\ln(A_1/A_2)$ versus frequency when

22 G_1/G_2 is independent of frequency. To achieve the independence of G_1/G_2 from frequency, the

23 setting of sample dimensions, transducers and arrangements of test set-up for the reference

24 sample should be the same as that for the rock sample. When Q of the reference is sufficiently

25 high (i.e., $Q_1 \cong \infty$, and thus $\gamma_1 \cong 0$), γ_2 can be obtained from the slope of the fitting curve, and

26 hence Q of the rock sample can be determined. In this study, an aluminium sample with the

27 same dimensions as the rock sample was used as the reference to estimate Q values of jointed

28 rock samples because it has a much greater Q compared with the rock [39, 40]. The elastic

29 properties of the aluminium sample are given in Table 1 [41].

30

4. Results and analysis

4.1 Effects of fluid type and composition on wave propagation

Wave velocity

Fig. 4 shows the average wave velocities of single-liquid filled rock joints and corresponding jointed rock samples for incident P-waves with different central frequencies (i.e., 100 kHz and 1 MHz). Herein, single-liquid filled joints refers to the joints filled with air and one kind of liquid (i.e., water, BL10 or M68 in this study), including water-, BL10- and M68-filled joints. Figs. 4a and 4b illustrate that wave velocity of vertical water-filled joint increases with increasing volume content of filling water, which is consistent with previous observation from the natural rock joint filled with air and water [24]. Similar variations of wave velocities for light oil-filled rock joints and their corresponding jointed samples with increasing filling light oil content are also observed in Figs. 4a and 4b. In addition, for horizontal single-liquid filled joints, increasing volume content of filling liquid evidently leads to an increase in wave velocity when the liquid content is larger than 50%, as shown in Figs. 4c and 4d. The above observations indicate that, in most circumstances, higher filling liquid content in the joint results in higher wave velocity across the joint. On one hand, the Wood's law demonstrates that the effective bulk modulus of air-liquid layer is inversely proportional to the air volume content [26, 42]. Consequently, a higher liquid volume content, i.e., a decreasing air volume content, results in relatively larger bulk modulus of the joint, causing faster compressional wave velocity across the air-liquid filled joint. On the other hand, filling liquid introduces viscous coupling between two joint surfaces due to the inertia of liquid, thereby increasing bulk modulus of the joint [10]. The more filling liquid there is, the more significant viscous effect between rock matrix and the joint it is. Accordingly, a higher liquid content leads to an increase in bulk modulus of the joint, causing a higher wave velocity.

Moreover, Fig. 4 reveals that wave velocity of water-filled rock joint is higher than that of light oil-filled rock joint. This is mainly because that acoustic wave propagates faster in water due to its relatively larger bulk modulus of elasticity compared with light oils used in this study (see Table 2) [43]. It is also found that filling M68 in the joint results in a slightly higher wave velocity across the joint compared to BL10. This is because that viscosity of M68 is about six times larger than that of BL10 while the difference between their densities is negligible (as shown in Table 2). Consequently, filling M68 results in more significant coupling between rock matrix and the joint, thereby causing greater bulk modulus of the filled rock joint [44-45]. Besides, Fig. 4 demonstrates that liquid content in the single-liquid filled joint has more significant effects on wave velocity compared with the type of filling liquid, which could

9

be explained by the fact that bulk modulus of the joint varies drastically with volume content of filling liquid.

Fig. 5 shows wave velocities across dual-liquid filled joints and the corresponding jointed rock samples at different wave frequencies (i.e., 100 kHz and 1 MHz). In this study, dual-liquid filled rock joints are divided into two categories, i.e., water-BL10 filled joint that is fully filled with water and BL10, and water-M68 filled joint which is fully filled with water and M68. As water content in the dual-liquid joint increases, a nonlinear increase in wave velocity could be observed. Additionally, wave velocity of water-M68 filled joint is higher than that of water-BL10 filled joint. It is mainly because the bulk modulus of M68 is larger than that of BL10, causing higher bulk modulus of the water-M68 layer compared to the water-BL10 layer. These findings further indicate that filling water results in higher wave velocity of rock joint compared to light oils, while filling M68 instead of BL10 could lead to faster wave propagation across the joint.

Results in Figs. 4 and 5 indicate that different from single-liquid filled rock joints, the increase in wave velocity across dual-liquid filled joints with changing liquid composition in the joint is small. It is probably because that, compared with single-liquid filled joints, dual-liquid filled joints are always fully filled with liquids. Thus, variation of filling liquid composition has small effects on the bulk modulus and density of the filled joint. Moreover, tendencies of wave velocity in jointed rock samples resemble those of wave velocity across their corresponding fluid-filled rock joints, implying that wave velocity of jointed rock masses is dominated by individual fluid-filled rock joints.

Transmission coefficient

Based on Eq. (4), the transmission coefficients for P-wave propagation through the single-liquid filled joints are calculated and plotted as a function of liquid content in the joint, as shown in Fig. 6. Figs. 6a and 6b illustrate that increasing water content in vertical rock joints significantly improves wave transmission across the joint, which is in accordance with findings in Yang et al. [10]. The similar trends of transmission coefficients across M68- and BL10-filled joints caused by the growth of liquid content were also observed. In addition, under certain conditions, the larger filling liquid content in horizontal rock joints could also results in more wave transmission, as shown in Figs. 6c and 6d. The main reason for these findings is that wave impedance of air is much lower than those of rock matrix and filling liquid [46]. Thus, wave reflection at the air-rock interface decreases by the reducing interface area due to the increase of filling liquid content. Besides, the specific stiffness of the joint [10] increases with

the growth of fractional contact area between liquid and rock matrix caused by the rising liquid content, which could enhance wave transmission across the joint [47]. Fig. 6 also reveals that transmission coefficients across water-filled rock joints are larger than those across light oil-filled joints under the same liquid content. It is because more wave energy transmission occurs at the water-rock interface due to the larger wave impedance of water compared to light oils [18]. Note that the wave impedance of a fluid is the product of wave velocity and density. Besides, energy loss of wave is less in water rather than oils because of smaller viscosity of water. Consequently, filling water results in larger transmission coefficients of wave across the whole joint. Additionally, at a given liquid content, transmission coefficient is slightly larger when the joint is filled with BL10 rather than M68. It is mainly because that the viscosity of BL10 is evidently lower than that of M68 (see Table 2). Although a little more wave energy could transmit through the M68-rock interface compared to the BL10-rock interface, the increment is sufficiently small due to the tiny difference in wave impedance between those two oils. Since BL10 has a much smaller viscosity than M68, more wave energy can travel through BL10 rather than M68, which might compensate for the increment induced by the difference in wave impedance. Thus, filling BL10 leads to the larger total wave transmission across the joint.

Fig. 7 illustrates transmission coefficients for P-wave propagation through the dual-liquid filled joints as a function of water content. It is found that increasing water content in dual-liquid filled joints results in higher transmission coefficients, indicating that water allows more wave to transmit through the joint compared to light oils. In addition, at a given water content, transmission coefficients are slightly larger when BL10 rather than M68 exists in the joint, implying that BL10 allows more wave transmission compared to M68. These findings are consistent with the discrepancies in wave transmission between different single-liquid filled joints observed from Fig. 6. One possible explanation is that the wave impedance of water is greater than that of light oils used in this study. Specifically, the difference between wave impedances of rock matrix and water is the smallest, thus more wave energy transmits across the rock-water interface of the joint [18]. Apart from that, it could also be attributed to the contrast in liquid viscosity [17, 22, 48]. Viscosity of water is smallest among these three liquids, and viscosity of M68 is much greater than that of BL10, as shown in Table 2. Consequently, filling water results in the lowest wave absorption in the joint. Besides, BL10 leads to less wave energy loss across the joint compared to M68.

Frequency spectra

Fig. 8 presents frequency spectra of transmitted P-waves through single-liquid with different liquid contents. It is found from Figs.8a and 8c that the increasing volume content of filling liquid causes a noticeable increase in spectral amplitudes and a slight increase in the dominant frequency for vertical joints, which is in accord with previous findings (YANG et al., 2019). Similar variations of spectral contents caused by the increasing liquid content for horizontal joints with filling liquid content higher than 50% were also observed from Figs. 8b and 8d. Those findings could be attributed to that the rising liquid volume content leads to the higher wave velocity. Accordingly, the increased wave impedance of the air-liquid layer causes more wave energy transmission across the joint, and thus enhances the spectral amplitudes of transmitted signals [49]. Besides, Fig. 8 shows that the spectral amplitudes of transmitted waves through water-filled joints are larger than those of transmitted pulses across light oil-filled joints. It is because that more wave energy could transmit through water due to its larger wave impedance and smaller viscosity compared to light oils.

In addition, Figs. 8a and 8c shows that the dominant frequency slightly shifts to a greater value with the increase of liquid content when waves propagate through the vertical air-liquid filled joints. It is likely because the increasing liquid content results in an increase in the area of liquid-rock interface, causing more wave modes at high frequencies transmitting across the joint. The similar shape of frequency spectra and changes in the dominant frequency were observed for horizontal air-liquid filled joints with liquid contents of 75% and 100%, as illustrated in Figs. 8b and 8d. It is because that, like vertical joints containing liquids, horizontal joints with liquid content of 75% and 100% result in the partial or full connection between two joint surfaces through the filling liquid (due to surface tension to increase the surface level), generating the liquid-rock interface at all joint boundaries. As a result, waves mainly transmit into the joint through the liquid-rock interface at the joint surfaces. Consequently, the received transmitted pulses are mainly dependent on properties and volume contents of filling liquid.

By comparison, Figs. 8b and 8d show that the frequency spectra for horizontal joints with liquid contents of 25% and 50% are noticeably different from the above cases, which resemble the frequency spectrum for the horizontal joint without liquids (i.e., air-filled joints). It is because that, similar with the air-filled joint (i.e., liquid content is 0%), the free surface (i.e., air-rock interface) exists in horizontal joints with liquid contents of 25% and 50% (i.e., no enough surface tension effect to cause liquid-solid connection). To be specific, filling liquid only adheres to one joint surface while it cannot reach the other one for the liquid volume content of 25% or 50%. Thus, when waves impinge on those joints, the joint surface without

12

liquid would function as a free surface to reflect a significant portion of the incident wave energy. It is worthy to notice that a very small portion of wave may propagate along the surface of PMMA tube enclosed the joint. Accordingly, for horizontal joints with liquid contents of 0%, 25% and 50%, the frequency spectra of transmitted signals presumably result from surface waves transmitted by the PMMA tube. Additionally, Fig. 8 demonstrates that the type of filling liquid seldomly affects the dominant frequencies of spectra. It is likely because the difference in wave impedances among three liquids used in this study is small.

Fig. 9 shows spectral contents of transmitted P-waves through dual-liquid filled joints with different liquid compositions. It is observed that an increase in water content leads to larger spectral amplitudes of transmitted waves across water-oil filled rock joints. It is mainly attributed to the larger wave impedance and lower viscosity of water compared to oils. Besides, Fig. 9 reveals that the type and fraction of filling liquid exert few influences on the dominant frequencies and shapes of frequency spectra when waves propagate across the joint filled with water and one kind of oil. It is because that all dual-liquid filled joints are always fully saturated with liquids, causing entirely coupling between two joint surfaces through the filling liquids. Changes in liquid types and volume contents have less effects on wave impedance of the effective water-oil layer. Consequently, wave transmission across joints filled with the water-oil layer slightly changes, thereby scarcely altering the shape of frequency spectra. That is because that more high-frequency wave modes can transmit through liquid rather than air.

To further understand effects of fluid type and composition in rock joints on spectral contents, the maximum amplitudes of frequency spectra in Figs. 8 and 9 were summarized in Table 4. It shows that, for single-liquid filled joints at a given liquid content, the maximum amplitudes of transmitted waves across water-filled joints are the largest, followed by BL10-filled joints. Additionally, for dual-liquid filled joints with the same water content, joints containing BL10 result in larger maximum amplitudes compared to those filled with M68. These findings indicate that filling water allows more wave energy transmission across the rock joint compared to BL10 and M68, while BL10 transmits more wave energy than M68, which are consistent with findings in Figs.8 and 9. This is because water has a larger impedance and smaller viscosity than light oils, resulting in more wave energy transmission across the joint. Particularly, since the difference in impedance between M68 and BL10 is sufficiently small, their viscosities highly determine the discrepancy in total wave energy transmitted through joints. Moreover, compared with the dominant frequency, spectral amplitudes of transmitted waves become more sensitive to type and composition of filling liquid in the joint.

13

Q value

The average values and standard deviations of attenuation quality factor Q were calculated with Eq. (5) for rock samples with individual fluid-filled rock joints. Fig. 10 shows Q values of rock samples with single-liquid filled rock joint versus liquid content in joint. As liquid content in rock joint increases, Q values get greater regardless of the type of filling liquid. It indicates that the existence of liquid could reduce wave attenuation through single-liquid filled joints, which is consistent with laboratory results in Pyrak-Nolte et al. [10] and Yang et al. [24]. The reason is that the presence of liquid makes rock joints stiffer, allowing more wave energy transmission. It is also illustrated that the water-filled joint results in the greatest Q values, followed by the BL10-filled joint. It means that water-filled rock joints attenuate less wave energy than BL10- and M68-filled joints, and more wave attenuation occurs in M68-filled joints rather than BL10-filled joints. The observed small discrepancy in wave attenuation caused by different filling liquids could be attributed to the significant difference in viscosities of these liquids [17, 22, 48].

Fig. 11 presents Q values for rock samples with dual-liquid filled joints versus water content in the joint. It shows that increasing water content leads to greater Q values of rock samples with dual-liquid filled joints, implying that filling water reduce wave attenuation across the dual-liquid filled rock joints. It is also found that dual-liquid filled joints containing BL10 result in greater Q values than those filled with M68, suggesting that filling M68 attenuate more wave energy compared to BL10. These findings are in accordance with observations from different single-liquid filled rock joints shown in Fig. 10, which could also be explained by the differences in viscosities of liquids (i.e., water, BL10 and M68 in this study). More specifically, less wave energy is absorbed by filling water because of its lower viscosity compared to light oils.

4.2 Effects of joint orientation on wave propagation

Because of the flow characteristics of liquid, orientation of joint could affect the spatial distribution of filling fluids in the joint, thereby influencing wave propagation through the joint. Herein, the effects of joint orientation are analyzed to some extent based on experimental findings of wave attributes of vertical and horizontal joints.

1   *Wave velocity*

2   Fig. 4 illustrates that wave velocity of single-liquid filled rock joints is highly dependent on the

3   joint orientation. More specifically, for vertical single-liquid filled rock joint (see Figs. 4a and

4   4b), the wave velocity drastically increases when filling liquid content increases from 0% to

5   25%, followed by a continuous increase at a decreasing rate as liquid content gradually rises to

6   100%. By comparison, for horizontal single-liquid filled joint (see Figs. 4c and 4d), the wave

7   velocity seldom changes for liquid content below 50%, while it increases remarkably as liquid

8   content further rises from 50% to 100%. The discrepancy could be attributed to different effects

9   of fluid surface tension at various joint orientations [50-53]. Precisely, for vertical rock joints,

10   air and liquid are almost perfectly stratified along the joint surface, where the fluid tension at

11   the air-liquid interface has negligible influences on joint surface conditions. As a result, two

12   joint surfaces have the identical boundary which is comprised of the liquid-rock interface and

13   air-rock interface. Wave velocity mainly depends on the effective properties of the joint, which

14   highly affected by the volume content of liquid. On the contrary, for horizontal rock joints,

15   there is a critical value of liquid content, which depends on the air-liquid meniscus interface

16   caused by the surface tension, highly affects the boundary conditions of the joint surfaces [54].

17   To be specific, when filling liquid content exceeds the critical value, i.e., 75% and 100% in this

18   study, one joint surface is full covered by liquid while the other is partially wetted. Similar with

19   vertical joints containing liquids, wave velocity under those cases are strongly affected by

20   volume content of liquid. However, when filling liquid content is lower than the critical value,

21   i.e., 25% and 50%, filling liquid only adheres to one joint surface and the other is directly

22   exposed to the air. Thus, almost all of wave is reflected at the air-rock surface while a very

23   small portion of wave may propagate along the PMMA tube. Consequently, wave velocity

24   relies on material properties of the PMMA and hardly changes with increasing liquid content.

25   The critical value of filling liquid in a horizontal joint mainly depends on surface tensions at

26   the liquid-air-PMMA interface, which needs more tests to determine in future work.

27   For dual-liquid filled rock joints, the joint orientation has some minor effects on wave

28   velocity, as shown in Fig. 5. With increasing water content in dual-liquid rock joints, a

29   downward concave increase in wave velocity across vertical joints is observed in Figs. 5a and

30   5b, while an upward convex increase in wave velocity of horizontal joints is shown in Figs. 5c

31   and 5d. The minor discrepancy could be attributed to different effects of surface tension on

32   fluid distribution in vertical and horizontal dual-liquid filled joints. Specifically, two liquids

33   are purely stratified along the joint surface in vertical joints, while one liquid with smaller

34   content would form a pocket surrounded by the other liquid in horizontal joints. Consequently,

15

1   the effective elastic moduli of vertical joints mainly depend on elastic moduli of those two

2   liquids, while those of horizontal joints could also be affected by capillary pressure caused by

3   the inner liquid pocket in the joint.

4   Figs. 4 and 5 shows that, compared with single-liquid filled rock joints, changes in wave

5   velocities across dual-liquid filled joints caused by varying fluid composition are much smaller

6   regardless of the joint orientation. It is because that dual-liquid filled rock joints are always full

7   of liquids with small differences in the density and bulk modulus. Therefore, the evident

8   coupling and stiffening effects caused by filling liquids slightly change with fluid composition

9   in dual-liquid filled rock joints.

10

11   *Transmission coefficient*

12   As demonstrated in Figs. 6a and 6b, a relatively uniform increase in transmission coefficient

13   can be observed for the vertical single-liquid filled joint as liquid content gradually increases.

14   By contrast, for the horizontal single-liquid filled joint, transmission coefficient rarely changes

15   when the liquid content in joint is below 50%, while it sharply increases for the liquid content

16   in joint beyond 50%, as illustrated in Figs. 6c and 6d. These findings could be attributed to the

17   differences in joint surface conditions between vertical and horizontal joints. To be specific,

18   for a vertical joint, two joint surfaces are composed of air-rock and liquid-rock interfaces due

19   to the purely stratified distribution of air and liquid. Consequently, the increase of filling liquid

20   content directly results in larger area of liquid-rock interface, thereby enhancing wave

21   transmission across the joint. On the contrary, for a horizontal joint with the lower liquid

22   content (i.e., ≤ 50% in this study), one of its joint surfaces is the air-rock interface on which

23   almost all wave energy is reflected; and hence increasing liquid content has few effects on

24   wave transmission across the joint. When the liquid content exceeds a critical value (which is

25   between 50% and 75% in this study), two joint surfaces are connected through filling liquids,

26   generating the liquid-rock interface on all joint surfaces, which could highly enhance wave

27   transmission through the joint. As the liquid content further increases, the area of liquid-rock

28   interface becomes larger, causing an increase in wave transmission across the joint.

29   Regarding the dual-liquid filled joints (see Fig. 7), the consistent increasing trends of

30   transmission coefficients with increasing water content for both vertical and horizontal joint

31   orientations were observed. It indicates that the joint orientation has few effects on the

32   dependence of transmission coefficient of dual-liquid filled rock joints on the water content in

33   joint. This is mainly due to the fully saturated state of all dual-liquid filled joints at different

34   joint orientations, though the respective content of each of the two liquids in the joint is

different. It means that both surfaces of a joint are liquid-rock interfaces regardless of the joint orientation. Apart from that, elastic moduli and wave impedance of the joint slightly vary with fluid distribution modes because of small contrast in these parameters among water and two kinds of light oils in this study. As a result, changes in joint surface conditions caused by varying joint orientation have few effects on wave transmission across the joint.

Frequency spectra

For vertical single-liquid filled joints, increasing liquid content results in the increases of spectral amplitude and dominant frequency of transmitted waves, as shown in Figs. 8a and 8c. For horizontal single-liquid filled joints, similar trends of frequency spectra with increasing liquid content are observed only when liquid content is above 50% (Figs. 8b and 8d). When liquid content is lower than 50%, changing liquid content has negligible effects on frequency spectra. Furthermore, the joint orientation has significant effects on spectral contents for single-liquid filled rock joints with a fixed liquid content. For instance, with liquid content of 75%, spectral amplitudes for vertical joints are about three times larger than those for horizontal joints, and the dominant frequency for vertical joints is slightly higher than that for horizontal joints. These findings are consistent with observations from transmission coefficients, which further confirms that the liquid-rock interface on the joint surface determines wave transmission across the joint partially filled with liquid. Fig. 8 also illustrates that spectral amplitudes are much more sensitive to changing liquid content compared to the dominant frequency regardless of the joint orientation.

For dual-liquid filled rock joints, spectral amplitudes and the dominant frequency slightly increase with increasing water content regardless of joint orientation, as shown in Fig. 9. This implies that the joint orientation has few influences on spectral contents of transmitted waves across dual-liquid filled joints. It is in accordance with findings on transmission coefficients, which could also be attributed to the fact that dual-liquid filled joints are full of liquids regardless of the joint orientation. It can be concluded that changes in joint surface conditions caused by different joint orientation have much more significant effects on wave transmission across the joint compared to viscous effects of different filling liquids.

Q value

For rock samples with the vertical single-fluid filled joint, a continuously nonlinear increase in Q value is caused by the growth of liquid content, as shown in Figs. 10a and 10b. This means that wave attenuation could be significantly reduced by filling liquid in vertical joints. By

17

contrast, Q value for rock samples with the horizontal single-fluid filled joint almost stays constant with liquid content below 50%, while it increases dramatically with increasing liquid content when the liquid content is above 50% (see Figs 10c and 10d). It indicates that wave attenuation across horizontal joints decreases with increasing liquid content only when the liquid content exceeds a critical value. The above discrepancies in Q values between vertical and horizontal single-liquid filled joints are consistent with those in transmission coefficients.

By comparison, for rock samples with the dual-liquid filled joint, Q values consistently increase with water content in the joint regardless of the joint orientation, as illustrated in Fig. 11. It indicates that the increase of water content in dual-liquid joints gradually reduce wave attenuation no matter what the joint orientation is. Note that variations of Q values are in accordance with changes of transmission coefficients across the dual-liquid filled rock joints, which could also be attributed to the fact that varying joint orientation leads to minor variations of joint surface conditions when the joint is full of liquids. It is also found that the joint orientation induces relatively less influence on Q values caused by dual-liquid filled joints rather than single-liquid filled joints.

5. Discussion

5.1 Comparison with previous studies of fluid effects on wave propagation in rock masses

In this study, compressional wave behaviours across vertical joints filled with air and liquid are consistent with previous findings [24], which further confirms that wave attributes of the rock joint highly depend on weighted volumes of both liquid and air. In addition, for vertical rock joints filled with two types of liquids, wave velocity and wave transmission increase with the increasing volume content of fluid having relatively larger bulk modulus. By comparison, for horizontal joint filled with air and liquid, there is a critical liquid content (i.e., a value between 50% and 75% in this study) for the dependence of compressional wave properties on liquid content in the joint. When liquid content in rock joint is smaller than this critical value, wave behaviours across the joint resemble those through air-filled joint (i.e., open joint), that is, the presence of liquid has few influences on wave attributes of the joint. The discrepancies between wave behaviours across vertical and horizontal fluid-filled joints are similar with previous findings from rock containing micro-cracks saturated with water-oil [55]. These differences could be attributed to that wave responses to the joint depend on conditions of the fluid-rock interface that waves initially impinge on [55].

Furthermore, changes in wave properties of rock samples with individual fluid-filled joints caused by varying fluid composition are in accord with previous findings on rock masses

containing fluid-saturated micro-cracks/pore at high saturation degree [56-60]. The increase in wave velocity caused by the growth of volume content of the filling liquid with larger bulk modulus in the joint could be attributed to the fact that the increase in effective bulk modulus is much more significant than the increase in overall density of the joint [61]. The decreasing wave attenuation due to larger volume content of the filling liquid might because that filling liquid makes the joint stiffer and the difference in wave impedances between rock matrix and the joint smaller [62]. Similar with previous studies on rock masses containing fluid-saturated micro-cracks/pore [44, 51, 63], a strong dependence of wave attributes on the type of filling fluids in the joint is also observed in this study. The larger viscosity of fluid it is, the more wave attenuation caused by fluid-filled joint there is. It is also demonstrated that wave attenuation is much more sensitive to fluid-filled rock joints than wave velocity, which is consistent with observations from rock containing fluid-saturated microcracks/pores [64].

5.2 Interpretation from acoustics in fluids

In this study, the physical mechanisms for wave propagation in fluids, where fluid properties (including bulk modulus, density and viscosity) play significant roles, could be employed to account for wave behaviours across the fluid-filled rock joint. All rock joints tested in this paper are filled with two fluid phases; and hence the effective physical characteristics of those joints depend on the volume fractions and physical properties of two fluids. To be specific, following the Wood's law [65], the effective bulk modulus of the two-phase fluid layer in the joint can be obtained by

$$\frac{1}{K_{mix}} = \frac{\phi_{F1}}{K_{F1}} + \frac{\phi_{F2}}{K_{F2}} \tag{6}$$

where K_{F1} and K_{F2} are the bulk moduli of two different fluid phases, respectively; ϕ_{F1} and ϕ_{F2} are volume fractions of these two fluids in the joint, respectively. Based on Eq. (6), the bulk modulus of the two-phase fluid layer can be expressed in the form of [66]

$$K_{mix} = \frac{K_{F2}}{1 + \phi_{F1}\left(\dfrac{K_{F2}}{K_{F1}} - 1\right)} \tag{7}$$

Besides, according to the mass balance, the density of the two-phase fluid layer can be obtained via an arithmetic average of two fluid densities [67]

$$\rho_{mix} = \phi_{F1}\rho_{F1} + \phi_{F2}\rho_{F2} = \phi_{F1}\rho_{F1} + (1 - \phi_{F1})\rho_{F2} \tag{8}$$

where ρ_{F1} and ρ_{F2} are densities of two different fluid phases, respectively. Since the thin fluid-filled rock joint is analogous to a small section of fluid-filled thin-walled tube, wave velocity across the fluid-filled joint could be expressed in the form of [26]

$$V_{mix} = \frac{\sqrt{K_{F2}/\rho_{mix}}}{\sqrt{1 + K_{F2}\dfrac{D_t}{E_t e_t} + \phi_{F1}(\dfrac{K_{F2}}{K_{F1}} - 1)}} \tag{9}$$

where D_t and e_t are outer diameter and wall thickness of the tube, respectively; E_t is the elastic modulus of the tube material. It is worthy to notice that the formula takes the effect of the PMMA tube used for simulating fluid-filled joints into account. For rock joints filled with water and oil, with the increase of oil volume content (i.e., ϕ_{F1} in the formula), a more evident decrease in density of the two-phase fluid layer results in a higher wave velocity, which is consistent with observations from Fig. 5. For rock joints filled with air and liquid, recognizing that $K_{liq}/K_{air} \gg 1$ and $\rho_{liq}/\rho_{air} \gg 1$, wave velocity across the joint can be written as [68]

$$V_{mix} = \frac{\sqrt{K_{liq}/\rho_{mix}}}{\sqrt{1 + K_{liq}\dfrac{D_t}{E_t e_t} + \phi_{air}\dfrac{K_{liq}}{K_{air}}}} \tag{10}$$

where K_{liq} and K_{air} are bulk moduli of the liquid and air, respectively. The formula reveals that the decreasing air volume content, i.e., the increasing liquid volume content, drastically increases the value of K_{mix}, thereby enhancing wave velocity across the joint filled with air and liquid [66], which is in accordance with findings from Fig. 4.

Moreover, wave attenuation across fluid-filled rock joints is strongly affected by the fluid viscosity according to the mechanisms lying behind acoustics in fluids. Specifically, wave propagation in a fluid leads to a relative motion of adjacent layers of the fluid, causing viscous forces that act against the acoustic pressure due to the wave [69]. To overcome these viscous forces, energy is extracted from the wave, resulting in decrease in wave intensity (i.e., wave energy loss). Theoretically, the relationship between attenuation coefficient in a fluid and its viscosity could be expressed as [70]

$$\alpha = \frac{2\omega^2 \nu}{3\rho c^3} \tag{11}$$

where ω is angular frequency, ρ is density of the fluid, c is the phase velocity, and $\nu = \eta/\rho$ is the kinematic viscosity while η is the dynamic viscosity. It indicates that viscous loss in fluids is proportional to the fluid viscosity, which is the main reason for the finding that wave

attenuation in M68 is higher than that in BL10 and water. Based on the Grunberg-Nissan equation [71, 72], the viscosity of the two-phase fluid layer in the joint can be expressed as

$$\eta_{mix} = \eta_{F1} \left(\frac{\eta_{F2}}{\eta_{F1}} \right)^{\phi_{F2}} \tag{12}$$

The formula indicates that as the volume content of the more viscous fluid increases (i.e., ϕ_{F2} in the formula), the viscosity of two-phase fluid layer becomes larger, causing more wave energy loss. It is consistent with findings of wave attenuation across fluid-filled joints in this paper.

5.3 Influences of the incident wave frequency

As indicated by Yang et al. [24], the incident wave frequencies (bandwidth) have influences on wave attributes of individual fluid-filled rock joints. It is further confirmed by the comparison of wave properties between 100-kHz and 1-MHz incident P-waves propagation across various fluid-filled joints in this study. On the one hand, as illustrated in Figs. 4 and 5, wave velocity for 1-MHz incident P-wave is higher than that for 100-kHz incident P-waves. It is likely due to that higher-frequency waves tend to travel along faster paths and diffract around the heterogeneities when propagating through the fluid-filled joint [73]. Moreover, the finding is consistent with previous laboratory observations about wave velocity of rock containing fluid-saturated micro-cracks/pores, which could be explained by the local fluid flow theory [74, 75]. To be specific, filling liquids cannot relax immediately when higher frequency waves propagate across the joint, causing a larger bulk modulus and stronger shear effects of the joint.

On the other hand, wave transmission for 100-kHz input waves is slightly greater than that for 1-MHz input waves regardless of joint orientation as well as types and composition of filling liquids (see Figs. 6 and 7). Besides, frequency spectra in Figs. 8 and 9 show that the dominant frequency of 1-MHz P-waves evidently decreases, while it is almost unchanged for 0.1-MHz P-waves propagating across fluid-filled joints. It indicates that, similar with the rock joints having much smaller width than the wavelength, the relatively thicker fluid-filled rock joint could also behave as a low-pass filter. The explanation is that fluid viscosity has greater influences on higher-frequency waves than it does on lower-frequency waves. On one hand, wave at a higher-frequency results in motions of fluid particles at a faster rate, causing stronger molecular vibrations followed by more frictional heat due to the viscosity [76]. On the other hand, higher-frequency waves take longer paths than lower-frequency waves due to the multi-path effects, and hence they dissipate along a longer path [77].

21

Furthermore, Figs. 8 and 9 show that the dominant frequencies for transmitted 100-kHz and 1-MHz waves are about 120 kHz and 0.5 MHz, respectively. Herein, the dominant frequency for transmitted 100-kHz waves through jointed rock is larger than 100-kHz, which seems to violate the fact that the rock joint could act as a low-pass filter. It is presumably because that the exact dominant frequencies of signals generated by transducers used in this study are not equivalent to what the manufacturer marks. To support this explanation, an aluminum sample with the same dimensions as the jointed rock sample was tested to examine the exact dominant frequencies of incident pulses generated by ultrasonic transducers. The aluminum is chosen because it has been commonly used to calibrate ultrasonic test systems for its non-dispersive and non-attenuative properties [78]. The test results reveal that the exact dominant frequencies of signals produced by 100-kHz and 1-MHz transducers are about 140 kHz and 0.7 MHz, respectively. It means that the observations in Figs. 8 and 9 are not against the statement that the rock-fluid system could function as a low-pass filter on the propagating wave.

Moreover, to better understand wave behaviours across fluid-filled rock joints in time and frequency domains simultaneously, the time-frequency analysis was performed on received transmitted pulses in this study. Different from the spectral analysis, the time-frequency analysis describes how spectral contents of waves change with time [79]. Herein, the continuous-wavelet transform with a Morse wavelet was employed to generate time-frequency maps of transmitted waves across fluid-filled rock joints. Since similar trends of wave velocity and spectral contents have been observed from air-water and air-oil filled joints, the time-frequency analysis on air-water filled joints could be taken as an example to further demonstrate influences of air-liquid on wave propagation. Figs. 12 and 13 provide the typical time-frequency maps of transmitted 100-kHz and 1-Mhz P-waves across various air-water filled joints, respectively. It is found that almost no wave energy could transmit across empty joints (i.e., water content of 0%) regardless of the joint orientation, as shown in Figs. 12a, 12f, 13a and 13f. For normal wave incidence upon the vertical joints, transmitted wave energy increases with increasing liquid content regardless of the dominant frequency of input waves. Moreover, Figs. 12b-12e reveal that transmitted wave energy of 100-kHz input signals concentrates over the frequency range of 80 to 120 kHz, while Figs. 13b-13e indicate that transmitted wave energy of 1-MHz input signals concentrates in the frequency range from 0.3 to 0.7 MHz. By comparison, for normal wave incidence upon the horizontal joints, a small potion of wave energy transmits through the joints with water contents of 25% and 50%, followed by an increase in transmitted wave energy for water content of 75%. Besides, the

frequency ranges of energy concentration for horizontal joints with water content of 75% and 100% are similar with those for vertical joints. Overall, observations from Figs. 12 and 13 are consistent with findings of frequency spectra in Fig. 8, which further confirms the former analysis and conclusive results based on spectral analysis in this paper. Furthermore, Figs. 12 and 13 indicate that transmitted wave energy centers on the first arrival pulses, corresponding to the time range from 25 μs to 35 μs for 100-kHz input signals and the time range from 20 μs to 30 μs for 1-MHz input signals. The discrepancy between those two types of incident waves could be attributed to the dependence of wave velocity on wave frequency.

5.4. Implications and limitations

Nowadays, many acoustic techniques, e.g., vertical seismic profile, time-lapse seismic monitoring, cross-hole test, sonic well logging and ultrasonic imaging, have been widely applied to obtain detailed information about rock joints in the subsurface [80-84]. Results in the study could serve as a guidance for interpreting observations in many practical projects using acoustic techniques when the presence of fluid-filled rock joints is inevitable. For example, analyses of wave velocity and attenuation could provide useful information of physical properties and volume contents of fluids in rock joints. In addition, based on the dimensionless analysis, findings in this work could be upscaled for understanding seismic wave characteristics of shallow rock masses containing sparsely separated larger-scale fluid-filled joints (e.g., faults and fractures). Furthermore, the present study could compensate for laboratory documents about wave propagation and attenuation across fluid-filled rock joints, which might contribute to develop relevant wave theories in rock mechanics.

In this study, filling liquids in rock joint include water and two types of light oils, i.e., Shell Morlina S2 BL10 and Shell Tellus S2 M68. In nature, the rock joint could be filled with other kinds of liquids. Even so, the findings in this paper, in particular, the physical mechanisms lying behind and the dependence of acoustic behaviours on physical properties of fluids, are also applicable to the other fluid conditions. Only wave propagation across vertical (dip angle of 90°) and horizontal (dip angle of 0°) rock joints filled with fluids was investigated in this study. Nevertheless, the rock joints could be inclined, i.e., the dip angle is between 0° and 90° [85]. It is reasonably predicted that the seismic responses of inclined fluid-filled rock joints fall in between those of horizontal and vertical joints. Besides, this study only investigates wave propagation across singe fluid-filled rock joint. However, rock masses often consist of multiple joints, where joint spacing and joint number have significant influences on seismic wave behaviours [31, 86, 87]. So, it is necessary to investigate wave propagation in rock samples

23

with multiple fluid-filled joints in the future. Additionally, current study focuses on low-amplitude ultrasonic waves across fluid-filled rock joints where dynamic flow effect of filling fluids is negligible. In this regard, further investigation on high-amplitude shock wave propagation across fluid-filled rock joints is worthwhile to better understand the interaction between wave propagation and dynamic responses of the filling fluid in the joint. In addition, extra efforts are needed to study the impacts of the other environmental factors such as temperature, pressure, hydraulic and chemical conditions on wave propagation through fluid-filled rock joints.

6. Conclusions

In this paper, extensive ultrasonic tests have been performed to obtain deep insights into wave propagation and attenuation across individual fluid-filled rock joints. The results indicate that the type of filling liquids in rock joints plays an important role in seismic responses of jointed rock masses. Filling water results in faster wave propagation and more wave transmission compared to light oils. Acoustic behaviours across fluid-filled rock joints are mainly dependent on the elastic moduli and viscosity of filling fluids and variation in lumped wave impedance contrast of rock and fluids. In addition, compositions of fluids in individual rock joints, i.e., volume contents of air and liquid in single-liquid filled joints as well as volume contents of water and oil in dual-liquid filled joints, have significant influences on wave propagation across the joint. In most circumstances, increasing liquid content in a single-liquid filled joint enhances wave velocity and wave transmission. For dual-liquid filled rock joints, both wave velocity and wave transmission increase with increasing water content. Moreover, joint orientation strongly affects acoustic properties of rock joints partially filled with fluids while it has slight influences on wave propagation across fully fluid-filled joints. For vertical single-liquid filled joints, wave velocity and wave transmission drastically increase with rising liquid content. By comparison, for horizontal single-liquid filled joints, the liquid content could only dominate wave propagation and attenuation when it exceeds a critical value. Last but not least, seismic responses of fluid-filled rock joints are affected by the dominant frequency (bandwidth) of the incident waves. Both wave velocity and attenuation increase with the incident wave frequency.

References

[1] Cook NGW. Natural joints in rock: mechanical, hydraulic and seismic behaviour and properties under normal stress. Int. J. Rock Mech. Min. Sci. Geomech. Abstr. 1992;29(3):198-223.

[2] Soma N, Niitsuma H, Baria R. Estimation of deep subsurface structure in european hot dry rock test site, soultz-sous-forêts, france, by use of the AE reflection method. In: Proceedings of 25th Workshop on Geothermal Reservoir Engineering Stanford University. California; 24-26 January 2000. SGP-TR-165.

[3] Chavarria JA, Malin P, Catchings RD, Shalev E. A look inside the San Andreas fault at Parkfield through vertical seismic profiling. Science. 2003;302(5651):1746-8.

[4] De Matteis R, Vanorio T, Zollo A, Ciuffi S, Fiordelisi A, Spinelli E. Three-dimensional tomography and rock properties of the Larderello-Travale geothermal area, Italy. Phys. Earth Planet. Inter. 2008;168(1-2):37-48.

[5] Reshetnikov A, Buske S, Shapiro SA. Seismic imaging using microseismic events: Results from the San Andreas Fault System at SAFOD J. Geophys. Res. Solid Earth. 2010;115(B12): B12324.

[6] Reiser F, Schmelzbach C, Sollberger D, Maurer H, Greenhalgh S, Planke S, Kästner F, Flóvenz Ó, Giese R, Halldórsdóttir S, Hersir GP. Imaging the high-temperature geothermal field at Krafla using vertical seismic profiling. J. Volcanol. Geotherm. Res. 2018.

[7] Pyrak-Nolte LJ, Nolte DD. Approaching a universal scaling relationship between fracture stiffness and fluid flow. Nat. Commun. 2016;7:10663.

[8] Schoenberg M. Elastic wave behavior across linear slip interfaces. J. Acoust. Soc. Am. 1980;68(5):1516-21.

[9] Zhao J, Cai JG. Transmission of elastic P-waves across single fractures with a nonlinear normal deformational behavior. Rock Mech Rock Eng. 2001;34(1):3-22.

[10] Pyrak‑Nolte LJ, Myer LR, Cook NGW. Transmission of seismic waves across single natural fractures. J. Geophys. Res. 1990;95(B6):8617-38.

[11] Nagy PB. Ultrasonic classification of imperfect interfaces. J. Nondestruct. Eval. 1992;11(3-4):127-39.

[12] Brekhovskikh L. Waves in layered media. Elsevier; 2012.

[13] Rokhlin SI, Wang YJ. Analysis of boundary conditions for elastic wave interaction with an interface between two solids. J. Acoust. Soc. Am. 1991;89(2):503-15.

[14] Li JC, Wu W, Li HB, Zhu JB, Zhao J. A thin-layer interface model for wave propagation through filled rock joints. J Appl Geophys. 2013;91:31-8.

[15] Li JC, Li HB, Jiao YY, Liu YQ, Xia X, Yu C. Analysis for oblique wave propagation across filled joints based on thin-layer interface model. J Appl Geophys. 2014;102:39-46.

[16] Li JC, Li HB, Zhao J. Study on wave propagation across a single rough fracture by the modified thin-layer interface model. J Appl Geophys. 2014;110:106-14.

[17] Fehler M. Interaction of seismic waves with a viscous liquid layer. Bull. Seismol. Soc. Am. 1982;72(1):55-72.

[18] Zhu JB, Perino A, Zhao GF, Barla G, Li JC, Ma GW, Zhao J. Seismic response of a single and a set of filled joints of viscoelastic deformational behaviour. Geophys. J. Int. 2011;186(3):1315-30.

[19] Zhu JB, Zhao XB, Wu W, Zhao J. Wave propagation across rock joints filled with viscoelastic medium using modified recursive method. J Appl Geophys. 2012;86:82-7.

[20] Oelke A, Alexandrov D, Abakumov I, Glubokovskikh S, Shigapov R, Krüger OS, Kashtan B, Troyan V, Shapiro SA. Seismic reflectivity of hydraulic fractures approximated by thin fluid layers. Geophysics. 2013;78(4):T79-87.

[21] Minato S, Ghose R. AVO inversion for a non-welded interface: estimating compliances of a fluid-filled fracture. Geophys. J. Int. 2016;206(1):56-62.

[22] Place J, Ghafar AN, Malehmir A, Draganovic A, Larsson S. On using the thin fluid-layer approach at ultrasonic frequencies for characterising grout propagation in an artificial fracture. Int. J. Rock Mech. Min. Sci. 2016;89:68-74.

[23] Kamali-Asl A, KC B, Ghazanfari E, Hedayat A. Flow-induced alterations of ultrasonic signatures and fracture aperture under constant state of stress in a single-fractured rock. Geophysics. 2019;84(4):WA115-25.

[24] Yang H, Duan HF, Zhu JB. Ultrasonic P-wave propagation through water-filled rock joint: An experimental investigation. J Appl Geophys. 2019;169:1-14.

[25] Cengel YA, Boles MA. Thermodynamics: an engineering approach. McGraw Hill; 1998.

[26] Street RL, Watters GZ, Vennard JK. Elementary fluid mechanics. J. Wiley; 1996.

[27] Birch F. The velocity of compressional waves in rocks to 10 kilobars: 1. J. Geophys. Res. 1960;65(4):1083-102.

[28] ASTM Standard D2845-08. Standard test method for laboratory determination of pulse velocities and ultrasonic elastic constants of rock. ASTM International; 2008.

[29] Fratta D, Santamarina JC. Shear wave propagation in jointed rock: State of stress. Géotechnique. 2002;52(7):495-505.

[30] Wyllie MRJ, Gregory AR, Gardner LW. Elastic wave velocities in heterogeneous and porous media. Geophysics. 1956;21(1):41-70.

[31] Zhao J, Cai JG, Zhao XB, Li HB. Experimental study of ultrasonic wave attenuation across parallel fractures. Geomech. Geoeng. 2006;1(2):87-103.

[32] Achenbach J. Wave propagation in elastic solids. Elsevier; 2012.

[33] Nagata K, Nakatani M, Yoshida S. Monitoring frictional strength with acoustic wave transmission. Geophys. Res. Lett. 2008;35(6).

[34] Möllhoff M, Bean CJ, Meredith PG. Rock fracture compliance derived from time delays of elastic waves. Geophys. Prospect. 2009;58(6):1111-22.

[35] Nagata K, Kilgore B, Beeler N, Nakatani M. High-frequency imaging of elastic contrast and contact area with implications for naturally observed changes in fault properties. J. Geophys. Res. Solid Earth. 2014;119(7):5855-75.

[36] Stoica P, Moses RL. Spectral analysis of signals. Prentice Hall, 2005.

[37] Toksöz MN, Johnston DH, Timur A. Attenuation of seismic waves in dry and saturated rocks: I. Laboratory measurements. Geophysics. 1979;44(4):681-90.

[38] Johnston DH, Toksöz MN. Ultrasonic P and S wave attenuation in dry and saturated rocks under pressure. J. Geophys. Res. Solid Earth. 1980;85(B2):925-36.

[39] Zemanek Jr J, Rudnick I. Attenuation and dispersion of elastic waves in a cylindrical bar. J. Acoust. Soc. Am. 1961;33(10):1283-8.

[40] Johnston DH, Toksöz MN. Attenuation: a state-of-art summary, in: Johnston, Toksöz, editors. Seismic wave attenuation, S.E.G. Reprint Series No. 12, 1981. p. 123–35.

[41] Properties and selection: nonferrous alloys and special-purpose materials. ASM International: Handbook Committee; 1990.

[42] Wood AB. A textbook of sound: being an account of the physics of vibrations with special reference to recent theoretical and technical developments. G. Bell; 1955.

[43] Chaudhry MH. Applied Hydraulic Transients. Springer Science & Business Media; 2013.

[44] Wang ZJ, Nur A. Wave velocities in hydrocarbon-saturated rocks: Experimental results. Geophysics. 1990;55(6):723-33.

[45] Wang ZJ, Nur A. Ultrasonic velocities in pure hydrocarbons and mixtures. J. Acoust. Soc. Am. 1991;89(6):2725-30.

[46] Winkler KW, Murphy III WF. Acoustic velocity and attenuation in porous rocks. In Rock physics and phase relations: A Handbook of physical constants, AGU Reference Shelf (ed. Ahrens TJ). 1995:20-34.

[47] Petrovitch CL, Pyrak-Nolte LJ, Nolte DD. Combined scaling of fluid flow and seismic stiffness in single fractures. Rock Mech Rock Eng. 2014;47(5):1613-23.

[48] Wood AB. A textbook of sound: London, G. Bell and Sons, Ltd. 1949:361-2.

[49] Groenenboom J, Fokkema JT. Monitoring the width of hydraulic fractures with acoustic waves. Geophysics. 1998;63(1):139-48.

[50] Li X, Zhong LR, Pyrak-Nolte LJ. Physics of partially saturated porous media: Residual saturation and seismic-wave propagation. Annu. Rev. Earth Planet. Sci. 2001;29(1):419-60.

[51] Gurevich B. Effect of fluid viscosity on elastic wave attenuation in porous rocks. Geophysics. 2002;67(1):264-70.

[52] Liu ER. Effects of fracture aperture and roughness on hydraulic and mechanical properties of rocks: implication of seismic characterization of fractured reservoirs. J. Geophys. Eng. 2005;2(1):38-47.

[53] Dimri VP, Srivastava RP, Vedanti N. Reservoir Geophysics: Some Basic Concepts. In Handbook of Geophysical Exploration: Seismic Exploration. 2012;41: 89-118. Pergamon.

[54] Munson BR, Okiishi TH, Huebsch WW, Rothmayer AP. Fluid mechanics. Singapore: Wiley; 2013.

[55] Gist GA. Fluid effects on velocity and attenuation in sandstones. J. Acoust. Soc. Am. 1991;90(4):2370-1.

[56] O'Connell RJ, Budiansky B. Viscoelastic properties of fluid-saturated cracked solids. J. Geophys. Res. 1977;82(36):5719-35.

[57] Mavko GM, Nur A. Wave attenuation in partially saturated rocks. Geophysics. 1979;44(2):161-78.

[58] Winkler KW, Nur A. Seismic attenuation: Effects of pore fluids and frictional-sliding. Geophysics. 1982;47(1):1-5.

[59] Jones TD. Pore fluids and frequency-dependent wave propagation in rocks. Geophysics. 1986;51(10):1939-53.

[60] Knight R, Nolen-Hoeksema R. A laboratory study of the dependence of elastic wave velocities on pore scale fluid distribution. Geophys. Res. Lett. 1990;17(10):1529-32.

[61] Cadoret T, Marion D, Zinszner B. Influence of frequency and fluid distribution on elastic wave velocities in partially saturated limestones. J. Geophys. Res. Solid Earth. 1995;100(B6):9789-803.

[62] Stein S, Wysession M. An introduction to seismology, earthquakes, and earth structure. John Wiley & Sons; 2009.

[63] Wang ZJ. Fundamentals of seismic rock physics. Geophysics. 2001;66(2):398-412.

[64] Winkler KW, Nur A. Pore fluids and seismic attenuation in rocks. Geophys. Res. Lett. 1979;6(1):1-4.

[65] Wood AB. A textbook of sound: being an account of the physics of vibrations with special reference to recent theoretical and technical developments. G. Bell; 1955.

[66] Larock BE, Jeppson RW, Watters GZ. Hydraulics of pipeline systems. CRC press; 1999.

[67] Batzle M, Wang ZJ. Seismic properties of pore fluids. Geophysics. 1992;57(11):1396-408.

[68] Wylie EB, Streeter VL. Fluid transients in systems. Englewood Cliffs, NJ: Prentice Hall; 1993.

[69] Trevena DH. Ultrasonic waves in liquids. Contemp. Phys. 1969;10(6):601-14.

[70] Elmore WC, Heald MA. Physics of waves. Courier Corporation; 1985.

[71] Teja AS, Rice P. Generalized corresponding states method for the viscosities of liquid mixtures. Ind. Eng. Chem. Fundam. 1981;20(1):77-81.

[72] Rubino JG, Holliger K. Seismic attenuation and velocity dispersion in heterogeneous partially saturated porous rocks. Geophys. J. Int. 2012;188(3):1088-102.

[73] Louati M, Ghidaoui MS. High-frequency acoustic wave properties in a water-filled pipe. Part 1: Dispersion and multi-path behaviour. J. Hydraul. Res. 2017;55(5):613-31.

[74] Cadoret T, Marion D, Zinszner B. Influence of frequency and fluid distribution on elastic wave velocities in partially saturated limestones. J. Geophys. Res. Solid Earth. 1995;100(B6):9789-803.

[75] Mavko G, Vanorio T. The influence of pore fluids and frequency on apparent effective stress behavior of seismic velocities. Geophysics. 2010 Jan;75(1):N1-7.

[76] Radziuk D, Möhwald H. Ultrasonically treated liquid interfaces for progress in cleaning and separation processes. Phys. Chem. Chem. Phys. 2016;18(1):21-46.

[77] Louati M, Ghidaoui MS. High-frequency acoustic wave properties in a water-filled pipe. Part 2: range of propagation. J. Hydraul. Res. 2017;55(5):632-46.

[78] ASTM E127-07. Standard Practice for Fabricating and Checking Aluminum Alloy Ultrasonic Standard Reference Blocks, ASTM International, West Conshohocken, PA, 2007.

[79] Daubechies I. The wavelet transform, time-frequency localization and signal analysis. IEEE Trans. Inf. Theory 1990;36(5):961-1005.

[80] Yin X, Zong Z, Wu G. Research on seismic fluid identification driven by rock physics. Sci. China Earth Sci. 2015;58(2):159-71.

[81] Lumley DE. Time-lapse seismic reservoir monitoring. Geophysics. 2001;66(1):50-3.

[82] Pratt RG, Worthington MH. The application of diffraction tomography to cross-hole seismic data. Geophysics. 1988;53(10):1284-94.

[83] Cheng CH, Toksöz MN, Willis ME. Determination of in situ attenuation from full waveform acoustic logs. J. Geophys. Res. Solid Earth. 1982;87(B7):5477-84.

[84] Davatzes NC, Hickman SH. Stress, fracture, and fluid-flow analysis using acoustic and electrical image logs in hot fractured granites of the Coso geothermal field, California, USA. In: Pöppelreiter, M.,García-Carballido,C., Kraaijveld,M.(Eds.), Dipmeter and Borehole Image Log Technology.AAPG Memoir. 2010;92; 259-293.

[85] Liu X, Han G, Wang E, Wang S, Nawnit K. Multiscale hierarchical analysis of rock mass and prediction of its mechanical and hydraulic properties. J. Rock Mech. Geotech. Eng. 2018;10(4):694-702.

[86] Zhu JB, Zhao X, Li JC, Zhao G, Zhao J. Normally incident wave propagation across a joint set with the virtual wave source method. J Appl Geophys. 2011;73(3):283-8.

[87] Wu W, Zhu JB, Zhao J. A further study on seismic response of a set of parallel rock fractures filled with viscoelastic materials. Geophys. J. Int. 2013;192(2):671-5.

Herein, T refers to the transmission coefficient. Note that the dual-liquid filled joint is fully filled with two kinds of liquids among water, BL10 and M68.

Fig. 8 Frequency spectra of transmitted waves through rock samples with different liquid volume content in single-liquid filled joints: 100-kHz P-waves across (a) vertical and (b) horizontal joints; 1-MHz P-waves across (c) vertical and (d) horizontal joints. Note that the single-liquid filled joint is filled with one kind of liquids among water, BL10 and M68. For water- filled joints, P_L represents volume content of water; for BL10-filled joints, P_L stands for volume content of BL10; for M68-filled joints, P_L refers to volume content of M68.

Fig. 9 Frequency spectra of transmitted waves through rock samples with dual-liquid filled joints: 100-kHz input waves through (a) vertical and (b) horizontal joints; 1-MHz input waves through (c) vertical and (d) horizontal joints. Note that the dual-liquid filled joint is fully filled with two kinds of liquids among water, BL10 and M68. P_W represents volume contents of water while P_O refers to volume contents of light oil (BL10 or M68).

Fig. 10 Attenuation quality factor Q of rock samples with single-liquid filled rock joints versus liquid content in rock joint: (a) and (b) for 100-kHz and 1-MHz incident P-waves across vertical joints, respectively; (c) and (d) for 100-kHz and 1-MHz incident P-waves across horizontal joints, respectively. Note that the single-liquid filled joint is filled with one kind of liquids among water, BL10 and M68.

Fig. 11 Attenuation quality factor Q of rock samples with dual-liquid filled rock joints vs water content in rock joint: (a) and (b) for 100-kHz and 1-MHz incident P-waves across vertical joints, respectively; (c) and (d) for 100-kHz and 1-MHz incident P-waves across horizontal joints, respectively. Note that the dual-liquid filled joint is fully filled with two kinds of liquids among water, BL10 and M68.

Fig. 12 Time-frequency maps for 100-kHz P-waves transmitted through air-water filled rock joints with different water contents: (a) - (e) vertical rock joints, (f) - (j) horizontal joints. Herein, P_W stands for water volume content in the joint.

Fig. 13 Time-frequency maps for 1-MHz P-waves transmitted through air-water filled rock joints with different water contents: (a) - (e) vertical rock joints, (f) - (j) horizontal joints. Herein, P_W stands for water volume content in the joint.

Table 1. Physical and mechanical properties of materials used in the study

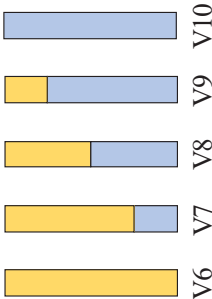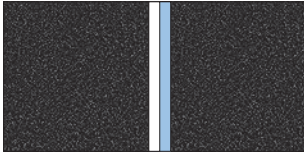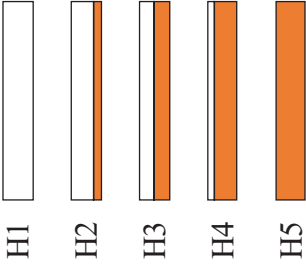| Material type	Density (kg/m³)	Young's modulus (GPa)	Poisson's ratio	Porosity (%)	P-wave velocity (m/s)	
					$f_1 = 100$ kHz	$f_2 = 1$ MHz
Gabbro rock	2818.82	100.36	0.29	1.31	5895.49 ± 13.63	5954.07 ± 4.22
Aluminium	2700.00*	69.00*	--	--	6322.09 ± 18.06	6369.53 ± 1.85

*Adopted from [40].
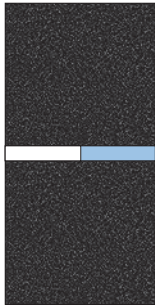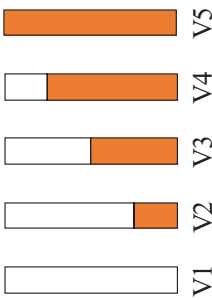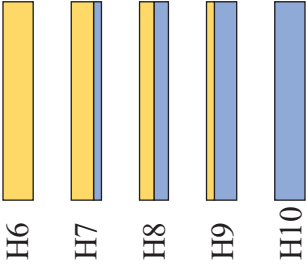
Table 2. Properties of filling fluids at room temperature (about 20 ℃)

Fluids	Density (kg/m^3)	Viscosity (kg/m·s)	Bulk modulus (GPa)
Air *	1.204	1.825×10^{-5}	0.101×10^{-3}
Water $^{++}$	998.2	1.002×10^{-3}	2.105
Shell Morlina S2 BL10	872.5	31.86×10^{-3}	1.683
Shell Tellus S2 M68	875.1	178.3×10^{-3}	1.748

* Adopted from [25].

$^{++}$ Adopted from [26].

Table 3. Horizontal and vertical fluid-filled joints under different filling conditions in this study

Types of jointed rock sample	Single-liquid filled joints	Dual-liquid filled rock joints	Fluid filling conditions
Rock sample with single vertical fluid-filled joint	V1 V2 V3 V4 V5	V6 V7 V8 V9 V10	**V1 & H1**: P_W (or P_O) = 0% **V2 & H2**: P_W (or P_O) = 25% **V3 & H3**: P_W (or P_O) = 50% **V4 & H4**: P_W (or P_O) = 75% **V5 & H5**: P_W (or P_O) = 100%
Rock sample with single horizontal fluid-filled joint	H1 H2 H3 H4 H5	H6 H7 H8 H9 H10	**V6 & H6**: P_W = 0%, P_O = 100% **V7 & H7**: P_W = 25%, P_O = 75% **V8 & H8**: P_W = 50%, P_O = 50% **V9 & H9**: P_W = 75%, P_O = 25% **V10 & H10**: P_W = 100%, P_O = 0%

Note: P_W and P_O represent volume contents of water and light oil (Shell Morlina S2 BL10 or Shell Tellus S2 M68) relative to the whole volume the open rock joint, respectively.

Table 4. Maximum amplitudes of frequency spectra for transmitted waves through rock samples with different fluid-filled joints

P_L	Input waves	Joint orientation	Maximum amplitudes (V)				
			Single-liquid filled joints			Dual-liquid filled joints	
			water	BL10	M68	water-BL10	water-M68
25%	$f_1 =$ 100kHz	V	0.0051	0.0049	0.0046	0.0276	0.0273
		H	0.0047	0.0046	0.0045	0.0267	0.0266
	$f_2 = 1$MHz	V	0.0333	0.0274	0.0267	0.2040	0.1953
		H	0.0017	0.0014	0.0012	0.1725	0.1702
50%	$f_1 =$ 100kHz	V	0.0123	0.0110	0.0010	0.0287	0.0281
		H	0.0039	0.0036	0.0036	0.0274	0.0273
	$f_2 = 1$MHz	V	0.1368	0.1254	0.0951	0.2117	0.2025
		H	0.0014	0.0014	0.0013	0.1774	0.1762
75%	$f_1 =$ 100kHz	V	0.0228	0.0202	0.0192	0.0293	0.0288
		H	0.0116	0.0107	0.0103	0.0287	0.0285
	$f_2 = 1$MHz	V	0.1984	0.1716	0.1617	0.2162	0.2133
		H	0.0642	0.0563	0.0472	0.1828	0.1798
100%	$f_1 =$ 100kHz	V	0.0312	0.0273	0.0267	0.0312	0.0312
		H	0.0311	0.0261	0.0253	0.0311	0.0311
	$f_2 = 1$MHz	V	0.2205	0.1962	0.1874	0.2205	0.2205
		H	0.1956	0.1649	0.1633	0.1956	0.1956

Note: H and V stand for horizontal and vertical directions, respectively. For single-liquid filled joints, P_L represents volume contents of water, BL10 or M68. For dual-liquid filled joints, P_L refers to volume contents of water in the joint.